SUPPLEMENTARY MATERIAL

PDGFRA Regulates Proliferation of Gastrointestinal Stromal Tumor Cells with Mutations in *KIT* by Stabilizing ETV1

Yujiro Hayashi, Michael R. Bardsley, Yoshitaka Toyomasu, Srdjan Milosavljevic, Gabriella B. Gajdos, Kyoung Moo Choi, KMarie Reid-Lombardo, Michael L. Kendrick, Juliane Bingener-Casey, Chih-Min Tang, Jason K. Sicklick, Simon J. Gibbons, Gianrico Farrugia, Takahiro Taguchi, Anu Gupta, Brian P. Rubin, Jonathan A. Fletcher, Abhijit Ramachandran, Tamas Ordog

Correspondence: Tamas Ordog, M.D., Mayo Clinic, Guggenheim 10, 200 1st Street SW, Rochester, MN 55906 USA. Email : ordog.tamas@mayo.edu, phone: (507) 538-3906, fax: (507) 255-6318

This file contains the following:

SUPPLEMENTARY METHODS

Materials

Crenolanib besylate and imatinib mesylate were from AROG Phamaceuticals (Dallas, TX) and LC Laboratories (Woburn, MA), respectively. MG132, PD98059 and cycloheximide were from Calbiochem (EMD Millipore, Billerica, MA); dimethyl sulfoxide (DMSO), puromycin and Triton X-100 were from Sigma-Aldrich (St. Louis, MO).

KIT and PDGFRA immunohistochemistry

Human formalin-fixed, paraffin-embedded (FFPE) GIST samples were processed and analyzed in two cohorts.

Cohort 1: 20 FFPE GIST samples (see **Supplementary Table S1** for demographic and clinicopathological information) were sectioned at 4-6 μm thickness and processed for PDGFRA and KIT immunohistochemistry using Leica BOND-III fully automated stainer and diaminobenzidine chemistry. The following reagents were used: Novocastra Bond Epitope Retrieval Solution 2 (EDTA, pH9; 20min), Bond Antibody Diluent (Leica AR9352), Polymer Refine Detection Kit (Leica DS9800), Leica DAB Kit and hematoxylin counterstain. The rabbit monoclonal anti-human PDGFRA antibody (Cell Signaling Technology #5241; clone: D13C6) was applied at 1:400 dilution for 30 min; the rabbit polyclonal anti-human KIT antibody (Dako A4502) was applied at 1:500 dilution for 15 min. Human breast cancer, GIST and tonsil tissues were used as staining controls. Blind scoring of PDGFRA immunoreactivity was performed by a clinical pathologist not involved in the study. Genotyping of the same tissues for common *KIT* and *PDGFRA* mutations was performed by Sanger sequencing by the Mayo Clinic Department

of Pathology and Laboratory Medicine Molecular Anatomic Pathology Laboratory Research Service. Images were captured with an Olympus (Center Valley, PA) BX51 microscope equipped with a UPlanFl 40×, 0.75 NA air objective and an Olympus DP72 color camera.

Cohort 2: FFPE GIST samples (23 different tumors from 21 patients; see **Supplementary Table S2** for demographic and clinicopathological information) were stained and analyzed as above with the following modifications: PDGFRA staining was performed using Leica BOND-RX fully automated stainer. KIT immunostaining was performed by Dr. Brian P. Rubin at the Cleveland Clinic using CC1 epitope retrieval for 32 min on a Ventana Benchmark stainer. The Dako A4502 antibody was applied at 37 °C for 16 min.

Fresh frozen samples of murine gastric corpus were sectioned at 12 μm and labeled with rat monoclonal anti-Pdgfra and goat polycloncal anti-Kit primary antibodies (4°C overnight) and fluorescent-tagged secondary antibodies (see **Supplementary Table S7** for details) following previously established protocols.[1,2] 12-bit images were acquired using a 40×, 0.75-NA oil immersion objective on an Olympus IX70 upright microscope. *Tunica muscularis* cells expressing one or both antigens and containing a DAPI-labeled nucleus were quantified using Adobe (San Jose, CA) Photoshop CS5 Extended version.

Multi-parameter flow cytometry analysis of murine interstitial cells of Cajal (ICC) and ICC stem cells (ICC-SC)

Murine ICC and ICC-SC were identified in the hematopoietic marker-negative fraction of dissociated gastric corpus+antrum tunica muscularis as $Kit^{+}Cd44^{+}Cd34^{-}$ and $Kit^{low}Cd44^{+}Cd34^{+}$ cells, respectively, using previously published protocols[3,4] with modifications (see **Supplementary Table S5** for detailed antibody information and **Supplementary Figure 1** for

gating scheme). Briefly, intact gastric corpus+antrum muscles were incubated with allophycocyanin (APC)-anti-Kit antibody (clone: ACK2) at 4°C for 3 h, then dissociated with collagenase digestion and trituration and filtered. Single-cell suspensions were incubated in 100 µL with anti-mouse Cd16/32 antibody (Fc block). Hematopoietic cells were identified with phycoerythrin (PE)-cyanine (Cy) 7-coupled anti-mouse Cd11b, anti-Cd45 and anti-F4/80 antibodies. Cells were also labeled with APC-anti-Kit (clone 2B8, which recognizes an epitope distinct from the epitope detected by ACK2), PE-anti-Pdgfra, eFluor 450- or fluorescein isothiocyanate (FITC)-anti-Cd34 and APC-Cy7-anti-mouse/human Cd44. Additional aliquots of the same samples were labeled in an identical manner but with appropriate isotype control antibodies. In experiments utilizing *Kit*$^{+/copGFP}$ mice expressing the copepod variant of green fluorescent protein (copGFP) from the endogenous *Kit* locus[5] or *Pdgfra*$^{+/eGFP}$ (B6.129S4-*Pdgfra*$^{tm11(EGFP)Sor}$/J) mice expressing the histone H2B-enhanced GFP (eGFP) fusion gene from the endogenous *Pdgfra* locus,[6] Kit^{+} and Pdgfra^{+} cells were identified by detecting copGFP and eGFP, respectively, in addition to immunostaining. In these studies, wild-type littermates were used as additional controls. Our experimental design was extensively verified by using single-stained and fluorescence-minus-one controls,[3,4] correlating immunolabeling- and GFP-based detection, as well as by sorting and detection of the ICC markers Kit and Ano1by real time reverse transcription—polymerase chain reaction (RT-PCR; not shown). Samples were analyzed using a Becton Dickinson (BD Bioscience, Franklin Lakes, NJ, USA) LSR II flow cytometer (see **Supplementary Table S6** for configuration) and FlowJo software (Treestar, Ashland, OR, USA).

Western blotting (WB)

Tissue and cell lysates were prepared and subjected to sodium dodecyl sulfate-polyacrylamide gel electrophoresis and immunoblotting as described previously[7] (see antibodies in **Supplementary Table S8**). Target and reference proteins were detected simultaneously using LI-COR Biosciences (Lincoln, NE) secondary antibodies tagged with near-infrared and infrared fluorescent dyes (IRDye700: red pseudocolor; IRDye800CW: green pseudocolor).[7]

RNA interference (RNAi)

RNAi against ETV1 and PDGFRA was performed using Dharmacon ON-TARGETplus® SMARTpool® small interfering RNA (siRNA) or corresponding scrambled sequences (25 nM) and DharmaFECT 4 Transfection Reagent (Thermo Fisher Scientific, Waltham, MA) according to the manufacturer's protocol. Treatment was applied following one-day culturing in antibiotic- and antimycotic-free media. Knock-down efficacy was assessed after 3 or 10 days by Western immunoblotting.

Cell viability analysis by methyl-tetrazolium salt (MTS) assay

One to three thousand cells per well were plated in complete media in 96-well flat-bottom plates. Cell viability was analyzed by the CellTiter 96® AQ_{ueous} Non-Radioactive Cell Proliferation Assay (Promega, Madison, WI) according to the manufacturer's protocol. Formazan absorbance data from the MTS assay were plotted as spline curves using SigmaPlot 10 (Systat Software, San Jose, CA). Drug concentrations producing 50% and 90% inhibition (IC_{50} and IC_{90}, respectively) were obtained from the dose-response curves.

Analysis of GIST cell proliferation by 5-ethynyl-2'-deoxyuridine (EdU) incorporation and propidium iodide (PI) labeling and flow cytometry

The Click-iT EdU Alexa Fluor (AF) 647 Flow Cytometry Assay Kit (Molecular Probes/Life Technologies; Thermo Fisher) was used according to the manufacturer's protocol with minor modifications. Briefly, EdU was added to cell culture medium to a final concentration of 10 μM for 60 min. After a wash, cells were harvested, pelleted at 500 *g* for 5 min and fixed for 15 min at room temperature with Click-iT fixative containing 4% paraformaldehyde. After washing and centrifugation, the cells were permeabilized with Click-iT saponin-based permeabilization buffer and incubated with 500 μL Click-iT reaction cocktail containing the AF 647 fluorochrome for 30 min at room temperature in the dark. After a wash with the Click-iT permeabilization buffer, the cells were incubated with 20 mg/mL ribonuclease A and PI staining solution (50 μg/mL) for 45 min at room temperature in the dark. Samples were analyzed using a Becton Dickinson LSR II flow cytometer (see **Supplementary Table S6** for configuration) and FlowJo software (Treestar). Chicken erythrocyte nuclei (used for checking instrument linearity) and calf thymocyte nuclei (BioSure, Grass Valley, CA) were used as controls.

Analysis of GIST cell proliferation by Ki-67 immunofluorescence

Imatinib-sensitive GIST-T1 or imatinib-resistant GIST-T1-5R cells were plated onto No. 1 coverslips coated with rat tail collagen (50,000 cells/coverslip) and maintained with complete growth media. After 24 h, the cells were treated with 8.3 (GIST-T1) or 33.2 nM (GIST-T1-5R) crenolanib or DMSO vehicle for 24 or 72 h. The cells were then washed, fixed with 4% paraformaldehyde for 10 min at room temperature, permeabilized with 0.3% Triton X-100 for 10

min at room temperature and blocked with 1% bovine serum albumin in phosphate-buffered saline pH 7.4 overnight at 4 °C. After labeling with anti-Ki-67 antibody (1:1,000 in blocking buffer; mouse IgG_1; clone 8D5; Cell Signaling Technology, Inc., Beverly, MA) at 4 °C overnight, the cells were washed and incubated with AF 594 goat anti-mouse IgG (5 μg/mL in blocking buffer; Molecular Probes/Life Technologies; Thermo Fisher) at room temperature for 30 min. Nuclei were counterstained with 4',6-diamidino-2-phenylindole (DAPI). Images were captured with a Nikon Eclipse TS-100F microscope (Nikon, Melville, NY) equipped with a Modulation Optics (Glen Cove, NY) 20× HMC ELWD Plan Fluor 0.45 NA air objective and a Jenoptik (Brighton, MI) ProgRes MFCool CCD camera.

Apoptosis assay

Twenty thousand cells per well were plated in complete media in 96-well flat-bottom plates. After 24h, drugs and fresh medium were added for 24 h. Apoptosis was evaluated by measuring caspase-3/7 activity by Caspase Glo-3/7 assay (Promega).

Chou-Talalay analysis

The combined effects of crenolanib besylate (AROG Pharmaceuticals, Dallas, TX) and imatinib on the viability of GIST-T1 cells were analyzed by the combination index (CI) method of Chou and Talalay.[8] Crenolanib, imatinib and crenolanib+imatinib were applied in triplicate at concentrations representing 0.25×, 0.5×, 1×, 2× and 4× of their individual IC_{50} (crenolanib: 6 nM; imatinib: 4 nM). 20 μM imatinib and 182 nM crenolanib were used as a positive control (100% inhibition) and dimethyl sulfoxide (DMSO) vehicle was used as negative control. CI was calculated using CompuSyn 1.0 software.

Retroviral transduction

Mouse wild-type *Kit* EcoRV/NotI fragment from pBluescript II phagemid vector (Agilent Technologies, Santa Clara, CA) was blunted and inserted into a blunt-end site (XhoI/HpaI) of pMSCV-PIG retroviral plasmid. Virus particles were produced using the Bosc23 cell line. 2XSCS2F10 cells were infected with 48- and 72-h supernatants and selected with increasing concentrations of puromycin followed by repeated immunomagnetic selection on Kit.[9] Homogeneity of GFP and Kit expression was verified by GFP fluorescence, immunofluorescent microscopy using chicken polyclonal anti-GFP (ab13970, Abcam, Cambridge, MA) and rat monoclonal anti-mouse Kit antibodies (ACK2 and 2B8, eBioscience, San Diego, CA), and flow cytometry.

Quantitative reverse transcription—polymerase chain reaction (qRT-PCR)

qRT-PCR was performed using previously published methods and specific, intron-spanning primers (Invitrogen, Carlsbad, CA).[4] The cDNA was amplified on a Bio-Rad CFX96 (Bio-Rad Life Science Research, Hercules, CA) real-time PCR detector using the SYBR GreenER qPCR SuperMix (Invitrogen).

GIST-T1 xenograft studies

Female adult athymic nude mice aged 6 weeks were maintained as described previously.[3] GIST-T1 cells were suspended in a 1:1 mixture of phosphate-buffered saline and growth factor-reduced Matrigel (Becton Dickinson) at a density of $3x10^6$ viable cells/100 μL. 200 μL cell suspension was injected subcutaneously in the left flanks. Tumor growth was assessed every

other day by measuring orthogonal diameters with an electronic caliper and calculating tumor volumes using the $4/3\times\pi\times((\text{length} + \text{width})/4)^3$ formula. Daily intraperitoneal treatments with 12.5 mg/kg crenolanib or DMSO vehicle were started when the tumor volumes reached 100 mm^3 and continued for 30 days. Tumor tissues and gastric *tunica muscularis* were snap frozen in liquid nitrogen and used for WB.

SUPPLEMENTARY TABLES

See next page for Supplementary Table S1.

Supplementary Table S1. Demographic and clinicopathological characteristics of GIST cases[a] (FFPE[b] samples; cohort 1)

Tissue	Age (yr)	Gender	Site	Histotype[c]	Neoadjuvant imatinib (mo)	Genotype[d]	PDGFRA staining score[e]
GIST-1	71	M	Stomach	E+S	-	KIT exon 11 c.1669_1674del p.W557_K558del	3
GIST-2	58	M	Stomach	E	-	KIT exon 11 c.1735_1737del p.D579del	0
GIST-3	59	F	Small intestine	S	-	KIT exon 11 c.1670_1678del p.W557_V560delinsF	2
GIST-4	49	F	Small intestine	E	-	KIT exon 11 c.1669T>A p.W557R	0
GIST-5	70	F	Abdomen	S	4	KIT exon 11 c.1676T>A p.V559D	3
GIST-6	82	M	Stomach	S	-	KIT exon 11 c.1655_1666del p.M552_Q556delinsK	1
GIST-7	58	M	Rectum	S	5	KIT exon 9 c.1504_1509dup p.A502_Y503dup; negative for KIT exon 11 mutation	3
GIST-8	68	F	Abdomen	S	7	KIT exon 11 c.1669_1674del p.W557_K558del	3
GIST-9	45	M	Rectum	S	6	KIT exon 11 c.1669_1674del p.W557_K558del	1
GIST-10	81	M	Stomach (fundus)	E	24	KIT exon 11 c.1674_1676del p.K558_V559delinsN	0/1[f]
GIST-11	74	M	Rectum	S	4	KIT exon 11 c.1679T>A p.V560D	3
GIST-12	82	M	Stomach	S	2	KIT exon 11 c.1654_1659del p.M552_Y553del	1
GIST-13	44	M	Abdomen	S+E	4	KIT exon 11 c.1669_1674del p.W557_K558del	3
GIST-14	71	M	Stomach	S	-	KIT exon 11 c.1727T>C p.L576P	3
GIST-15	45	F	Small intestine	S	-	Negative for KIT exon 9, 11, 13 & 17 and PDGFRA exon 12 & 18 mutations	3
GIST-16	45	F	Stomach	S	-	KIT exon 11 c.1679_1681del p.V560del; negative for KIT exon 9 mutation	3
GIST-17	61	F	GEJ[g]	S	4	KIT exon 11 c.1739_1753dup p.H580_F584dup	3
GIST-18	55	M	Abdomen	S	8	KIT exon 11 c.1650_1670del p.P551_W557del	3
GIST-19	52	M	Stomach	S	-	Failed (no DNA)	2
GIST-20	80	M	Stomach	S	-	KIT exon 11 c.1713_1739dup p.D579_H580ins9; negative for KIT exon 9 mutation	3

[a], FAM96A expression in the same samples was reported previously[10]; [b], FFPE, formalin-fixed, paraffin-embedded; [c], E, epithelioid; S, spindle-cell; [d], By PCR and sequencing; [e], Blind scores; scale: 0-3; [f], Focal cytoplasmic expression; [g], GEJ, gastroesophageal junction.

Supplementary Table S2. Demographic and clinicopathological characteristics of GIST cases (FFPE[a] samples; cohort 2)

Tissue	Age (yr)	Gender	Site	Histotype[b]	Neoadjuvant imatinib (mo)	Genotype[c]	PDGFRA staining score[d]
GIST-898	42	M	Stomach	S+E	-	N/A	3
GIST-900	54	F	Duodenum	S	-	N/A	1
GIST-901	71	M	Stomach	E+S	-	N/A	3
GIST-902	58	M	Stomach	E	-	N/A	0
GIST-903	59	F	Duodenum	S	-	N/A	3
GIST-904	59	F	Jejunum	S	-	N/A	1/0[e]
GIST-905	71	M	Abdomen	S+E	-	N/A	3
GIST-906	72	M	Stomach	S+E	-	N/A	3
GIST-907	70	M	Stomach	S	-	N/A	3
GIST-908	80	M	Stomach (fundus)	S	-	N/A	3
GIST-914	81	M	Stomach	E	13	N/A	1
GIST-909	49	F	Duodenum	S	-	N/A	1/0[e]
GIST-910	70	F	Stomach	S	5	N/A	3
GIST-911	78	M	Stomach	S	-	N/A	2
GIST-912	45	M	Rectum	S	-	N/A	3
GIST-915	50	F	Stomach	E+S	-	N/A	3
GIST-916	71	M	GEJ[f]	E+S	-	N/A	3
GIST-917	71	M	Stomach	S	-	N/A	3
GIST-918	45	F	Small intestine	S	-	Negative: KIT exon 9, 11, 13, 17 and PDGFRA exon 12 & 18	3
GIST-919	70	M	Stomach (fundus)	S	-	KIT exon 11 c.1655_1672del p.Met552_Trp557del; negative for KIT exon 9 mutation	3
GIST-920	45	F	Stomach	S	-	KIT exon 11 c.1679_1681del p.Val560del; negative for KIT exon 9 mutation	3
GIST-921	33	M	Jejunum	S	13+5 (7 mo no treatment)	KIT exon 11 c.1679_1681del p.Val560del; negative for KIT exon 9 mutation	0
GIST-922	61	F	Stomach	S	5	N/A	3

[a], FFPE, formalin-fixed, paraffin-embedded; [b], E, epithelioid; S, spindle-cell; [c], By PCR and sequencing; N/A, not available; [d], Blind scores; scale: 0-3; [e], Focal loss of expression; [f], GEJ, gastroesophageal junction. Blue boxes indicate samples that were from the same patients.

Supplementary Table S3. Demographic and clinicopathological characteristics of GIST cases (native samples; cohort 1)

Tissue	Age (yr)	Gender	Site	Size (cm; post-surgery)	Histotype	IHC[a]	Mitotic index	Risk[b]	Neoadjuvant imatinib (mo)	Notes
GIST-122	76	M	Stomach (distal)	7.4x5.8x5.1	Spindle	$KIT^{+}ANO1^{+}CD34^{+}$ $SMA^{c-}S100^{-}$	3/20 hpf[d]	Low (3.6%)	4	Stage IA lung cancer
GIST-320	82	F	Stomach (fundus)	5.0x3.6x 2.2	Unknown	KIT^{+}	2/50 hpf	Very low (1.9%)	-	
GIST-408	58	M	Distal esophagus, GEJ[e], proximal stomach	10.5x10.0x4.5	Spindle	$KIT^{+}CD34^{+}$ $SMA^{-}S100^{-}$ $KRT^{f}1\text{-}8,10,14\text{-}16^{-}$	10%	High	8	AJCC[g] stage ypT4N0M1
GIST-515	63	M	Stomach (lesser curve)	2.5x1.5x1.0	Spindle	$KIT^{+}SMA^{-}$	4/50 hpf	Very low	-	Single focus, pT2. Metastatic pancreatic cancer
GIST-730	92	F	Stomach (greater curve)	4.3x2.6x1.0	Spindle	$KIT^{+}ANO1^{+}DES^{h+}$ $MUC1^{i-}SMA^{-}$ $S100^{-}CD31^{-}$	1/50 hpf	Very low	-	Single focus, pT2pN0

[a], IHC, immunohistochemistry; [b], Risk of recurrence or progression by National Institutes of Health criteria; [c], SMA, smooth muscle actin (ACTG2); [d], hpf, high-power field; [e], GEJ, gastroesophageal junction; [f], KRT: cytokeratins detected by antibody cocktail AE1/AE3; [g], American Joint Committee on Cancer; [h]DES, desmin; [i], MUC1, mucin 1, cell surface associated (alias: EMA, epithelial membrane antigen)

Supplementary Table S4. Demographic and clinicopathological characteristics of GIST cases (native samples; cohort 2)

Tissue	Site	Neoadjuvant imatinib (Y/N)	Genotype
FX004.3	Stomach	N	KIT p.W557_K558>CE
003.7	Stomach	Y	KIT p.V560D
003.12	Stomach	N	KIT p.V559D
003.1	Small intestine	N	KIT exon 9 mutation
003.2	Small intestine	N	KIT exon 11 mutation

Supplementary Table S5. Antibodies used for flow cytometry analysis of cells freshly dissociated from murine gastric muscles

Target	Supplier	Host/Source	Clone/ID	Isotype	Label	Final conc. or µg/10^6 cells[a]
Cd16/32[b]	eBioscience	Rat mc[c]	93	IgG_{2a}, λ		1 µg
Cd11b[d]	eBioscience	Rat mc	M1/70	IgG_{2b}, κ	PE[e] -Cy7[f]	0.0312 µg
Cd45[g]	eBioscience	Rat mc	30-F11	IgG_{2b}, κ	PE-Cy7	0.0312 µg
F4/80[h]	eBioscience	Rat mc	BM8	IgG_{2a}, κ	PE-Cy7	0.0625 µg
Cd44[i]	BioLegend	Rat mc	IM7	IgG_{2b}, κ	APC[j]-Cy7	0.0625 µg
Kit	eBioscience	Rat mc	ACK2	IgG_{2b}, κ	APC	5 µg/mL
Kit	eBioscience	Rat mc	2B8	IgG_{2b}, κ	APC	0.25 µg
Cd34[k]	eBioscience	Rat mc	RAM34	IgG_{2a}, κ	eFluor 450 or FITC	0.2 µg
Pdgfra	eBioscience	Rat mc	APA5	IgG_{2a}, κ	PE	0.25 µg

[a], amount added to 100 µl of staining volume; [b], Cd16: Fc receptor, IgG, low affinity III; Cd32: Fc receptor, IgG, low affinity IIb; [c], mc, monoclonal; [d], Cd11b, integrin alpha M; [e], PE, phycoerythrin; [f], Cy7, cyanine 7; [g], Cd45, protein tyrosine phosphatase, receptor type, C; [h], F4/80, EGF-like module containing, mucin-like, hormone receptor-like sequence 1; [i], Cd44 antigen; [j], APC, allophycocyanin; [k], Cd34 antigen,. Suppliers: eBioscience, Inc., San Diego, CA; BioLegend, San Diego, CA

Supplementary Table S6. Configuration of the Becton Dickinson LSR II flow cytometer

Laser	Excitation wavelength (nm)	Dichroic filter (nm)	Emission filter (nm; peak/bandwith)	Detector type	Light scatter or fluorochromes used
Coherent® Sapphire™ 20 mW	488			Photodiode	Forward scatter
			488/10	PMT[a]	Side scatter
		505 LP[b]	530/30	PMT	FITC[c], copGFP[d], eGFP[e]
		550 LP	575/26	PMT	PE[f]
		595 LP	610/20	PMT	Unused
		685 LP	695/40	PMT	Unused
		735 LP	780/60	PMT	PE-Cy7[g]
Coherent® CUBE 100 mW	407		450/50	PMT	eFluor 450
		505LP	525/50	PMT	Unused
		535 LP	590/40	PMT	Unused
		595 LP	610/20	PMT	Propidium iodide
		630 LP	670/30	PMT	Unused
		670 LP	710/50	PMT	Unused
Coherent® CUBE 40 mW	640		660/20	PMT	APC[h], AF[i] 647
		685 LP	712/20	PMT	Unused
		735 LP	780/60	PMT	APC-Cy7

[a], PMT, photomultiplier tube; [b], LP, long-pass; [c], FITC, fluorescein isothiocyanate; [d], copGFP, copepod (*Pontellina plumata*) green fluorescent protein; [e], eGFP, enhanced GFP; [f], PE, phycoerythrin; [g], Cy7, cyanine 7; [h], APC, allophycocyanin; [i], AF, Alexa Fluor

Supplementary Table S7. Antibodies used in the mouse immunohistochemistry studies

Target	**Supplier**	**Host**	**Clone/ID**	**Isotype**	**Label**	**Final conc.**
Kit	RDS[a]	Goat pAb[b]	AF-1356	IgG		20µg/ml
Pdgfra	eBioscience[c]	Rat mAb[d]	APA5	IgG2a, κ		2µg/ml
Secondary Ab: Anti-goat IgG	Millipore[e]	Donkey pAb	AP180S		Cy5[f]	5µg/ml
Secondary Ab: Anti-rat IgG	Millipore	Donkey pAb	AP189C		Cy3[g]	2.5µg/ml

[a], RDS, R&D Systems, Inc., Minneapolis, MN; [b], pAb, polyclonal antibody; [c], eBioscience, Inc., San Diego, CA; [d], mAb, monoclonal antibody; [e], Millipore, Inc., Billerica, MA; [f], Cy5, cyanine 5; [g], Cy3, cyanine 3

Supplemental Table S8. Antibodies used in Western immunoblotting studies

Target	Supplier	Host	Clone/ID	Isotype	Label	Final conc.
GAPDH (h,m)[a]	Imgenex[b]	Goat pAb[c]	IMG-3073			0.05µg/mL
GAPDH (h,m)	Sigma[d]	Rabbit pAb	G9545			1:40000
GFP[e]	CST[f]	Mouse mAb[g]	4B10	IgG		1:2000
ERK1/2 (h,m)	CST	Mouse mAb	3A7	IgG1		1:4000
ETV1	Abcam[h]	Rabbit pAb	Ab81086			0.5µg/mL
Etv1 (m)	Thermo[i]	Rabbit pAb	PA5-19627	IgG		1:1000
KIT	Dako[j]	Rabbit pAb	A4520			1:4000
Kit (m)	RDS[k]	Goat pAb	AF1356			0.1µg/mL
KIT	SCBT[l]	Goat pAb	sc-1493			1:500
PDGFRA (h,m)	CST	Rabbit pAb	#3164			1:2000
PDGFRA	RDS	Goat pAb	AF-307-NA	IgG		0.1µg/mL
PDGFRB (h,m)	CST	Rabbit mAb	#4565	IgG		1:2000
P-ERK1/2 (T202/Y204 and T185/Y187)	CST	Rabbit mAb	197G2	IgG		1:1500
P-KIT (Y721)	CST	Rabbit pAb	#3391			1:2000
P-PDGFRA(Y742)	RDS	Rabbit pAb	AF2114	IgG		0.2 µg/ml
P-PDGFRB (Y1021)	BD	Mouse mAb	J105-412	IgG1, κ		0.5 µg/ml
Secondary Ab: Anti-rabbit IgG (H+L)[m]	LI-COR[n]	Donkey pAb	#926-32223		IRDye 680	1:10000
Secondary Ab: Anti-mouse IgG (H+L)	LI-COR	Donkey pAb	#926-32222		IRDye 680	1:10000
Secondary Ab: Anti-rabbit IgG (H+L)	LI-COR	Donkey pAb	#926-32213		IRDye 800CW	1:10000
Secondary Ab: Anti-goat IgG (H+L)	LI-COR	Donkey pAb	#926-32214		IRDye 800CW	1:10000

[a], h,m: used in both human and mouse cells/tissues; m: used in mouse cells/tissues only; all others: used in human cells only; [b], Imgenex Corp., San Diego, CA; [c], pAb, polyclonal antibody; [d], Sigma-Aldrich, Inc., St. Louis, MO; [e], GFP, green-fluorescent protein; [f], CST, Cell Signaling Technology, Inc., Beverly, MA; [g], MAb, monoclonal antibody; [h], Abcam plc, Cambridge, MA; [i], Thermo, Thermo Scientific, Pittsburgh, PA; [j], Dako North America, Inc., Carpinteria, CA; [k], RDS, R&D Systems, Inc., Minneapolis, MN; [l], SCBT, Santa Cruz Biotechnology, Inc., Dallas, TX; [m], H+L, highly cross-adsorbed; [n], LI-COR Biosciences, Lincoln, NE

SUPPLEMENTARY FIGURES

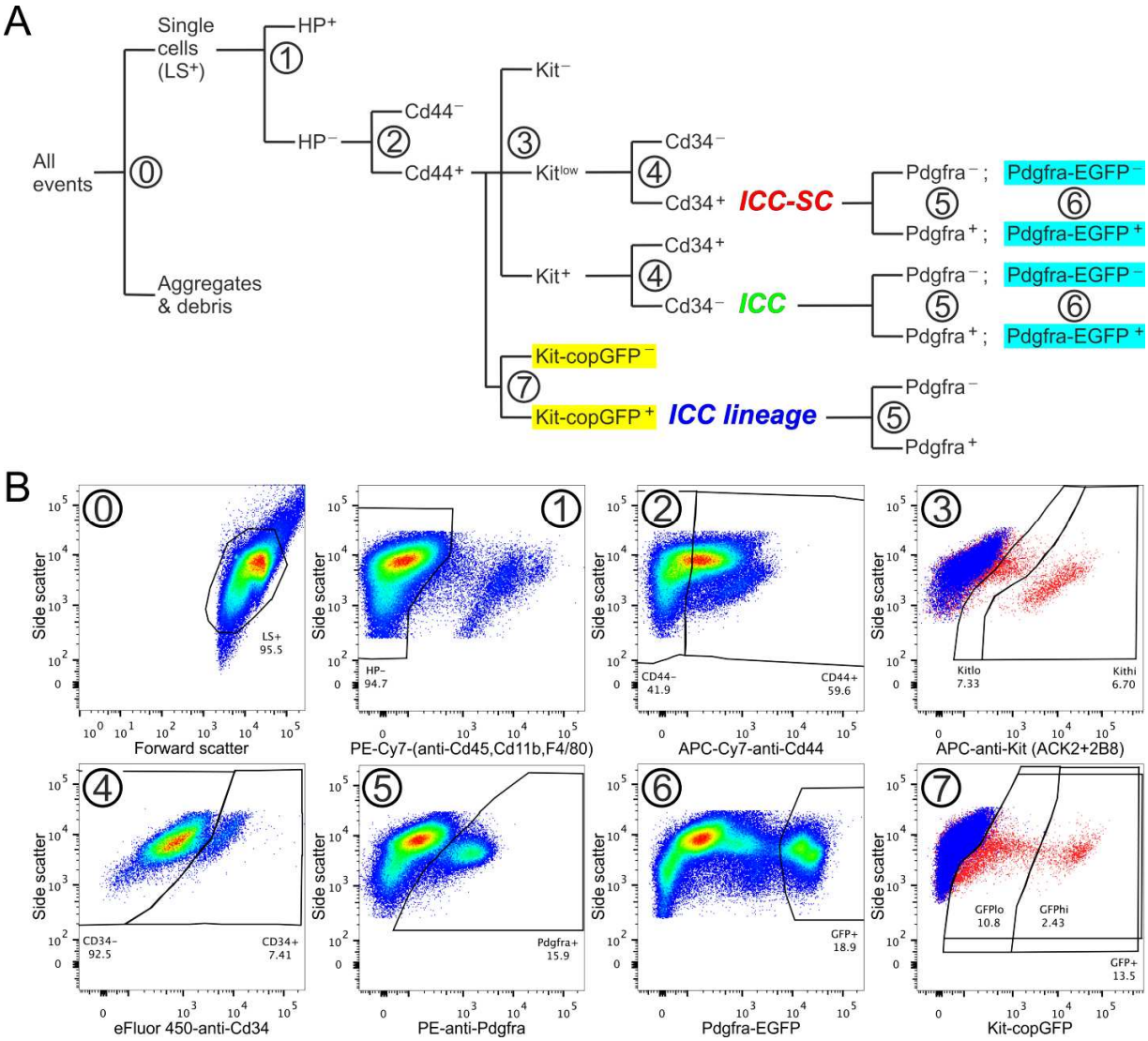

Supplementary Figure S1. Flow cytometry analysis of Kit and Pdgfra co-expression in the ICC lineage. (*A*) Gating sequence. ICC and ICC-SC were detected in the hematopoietic marker negative (HP^-) subset as $Kit^+Cd44^+Cd34^-$ and $Kit^{low}Cd44^+Cd34^+$ cells, respectively. In the experiments performed in $Kit^{+/copGFP}$ and $Pdgfra^{+/eGFP}$ mice, Kit- and Pdgfra-expressing cells were evaluated by copGFP and eGFP fluorescence, respectively, in addition to immunostaining. In the experiments utilizing $Kit^{+/copGFP}$ mice, Kit^+ ICC and Kit^{low} ICC-SC could not be reliably distinguished due to variable loss of cytoplasmic GFP during cell preparation (see below).

Therefore, Pdgfra expression was analyzed in the unfractionated ICC lineage (Kit-copGFP$^{low/+}$ cells). (*B*) Representative projections illustrating key cell populations identified by numbers in *A*. Population boundaries were determined on the basis of immunolabeling with appropriate pre-immune isotype control antibodies and drawn along lines representing identical cell counts in contour plots. Numbers in the two-dimensional projections indicate the proportion of cells within the specified clusters as percentages of the total cell count in the projection. ⓪: Cells with light scatter properties characteristic of single live cells (LS$^+$). ①: Separation of cells of hematopoietic origin (Cd45$^+$Cd11b$^+$F4/80$^+$ leukocytes; HP$^+$) from other components of the gastric muscles. ②: Identification of Cd44$^+$ cells in the HP$^-$ population. ③: Kit$^-$, Kit^{low} and Kit$^+$ cells determined by immunolabeling in the HP$^-$Cd44$^+$ parent population. ④: Identification of Cd34$^+$ and Cd34$^-$ cells. The same Cd34$^+$/Cd34$^-$ boundary was used to define Cd34$^+$ ICC-SC in the Cd44$^+$Kit^{low} population and Cd34$^-$ ICC in the Cd44$^+$Kit$^+$ population. ⑤: Identification of Pdgfra$^+$ cells by immunolabeling. ⑥: Identification Pdgfra$^+$ cells by nucleus-targeted eGFP fluorescence in *Pdgfra*$^{+/eGFP}$ mice. ⑦: Identification of Kit-expressing cells by cytoplasmic copGFP fluorescence in HP$^-$Cd44$^+$ populations of *Kit*$^{+/copGFP}$ mice. Note that in comparison to immunostaining (③), copGFP immunofluorescence severely underestimated the number of Kit$^+$ cells and overestimated the Kit^{low} fraction.

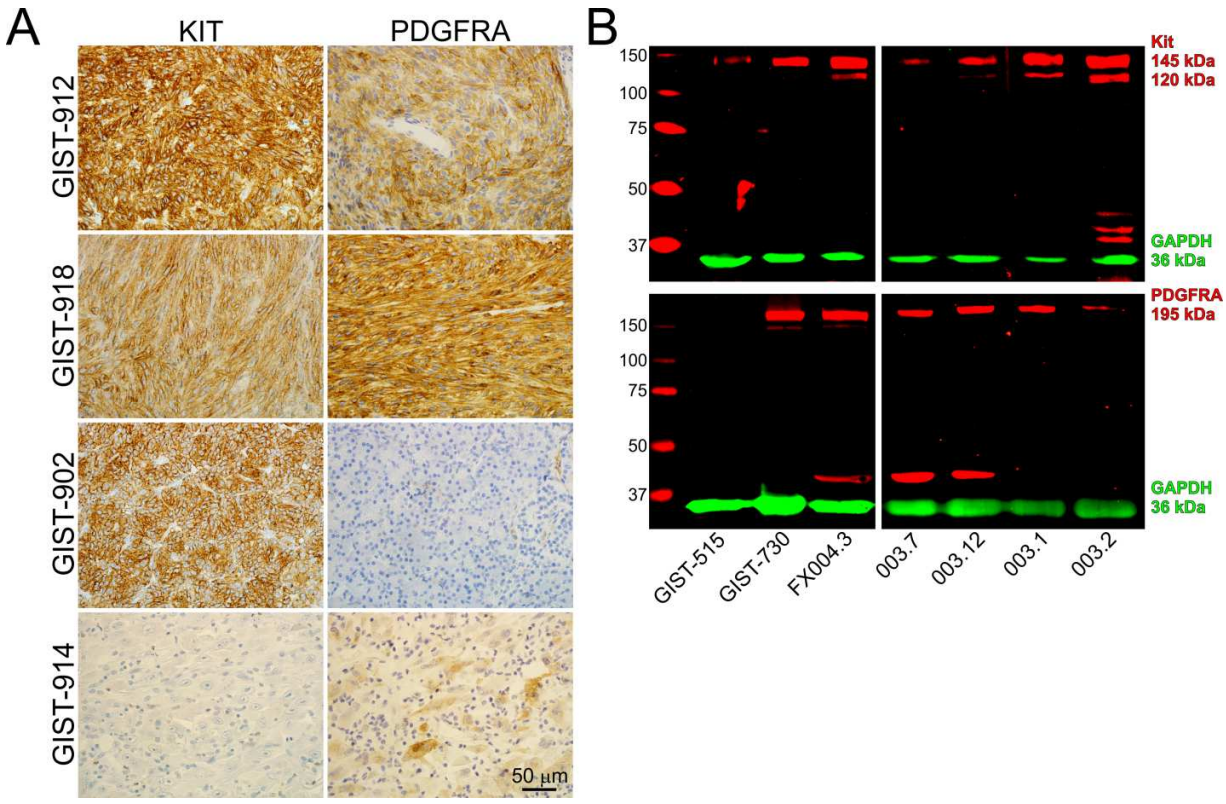

Supplementary Figure S2. Co-expression of KIT and PDGFRA in GIST. (*A*) KIT and PDGFRA expression (brown color) detected by immunohistochemistry in representative FFPE GIST samples from the cohort described in **Supplementary Table S2** (n=23 different tumors from 21 patients). Note samples with different expression profiles. (*B*) Profiling of KIT and PDGFRA expression in unfixed GIST samples by WB (see **Supplementary Tables S4 and S8** for details). Target proteins and GAPDH (loading control) were detected simultaneously using LI-COR Biosciences (Lincoln, NE) secondary antibodies tagged with near-infrared and infrared fluorescent dyes (IRDye700: red pseudocolor; IRDye800CW: green pseudocolor).[7] With the exception of GIST-515, all samples co-expressed KIT and PDGFRA.

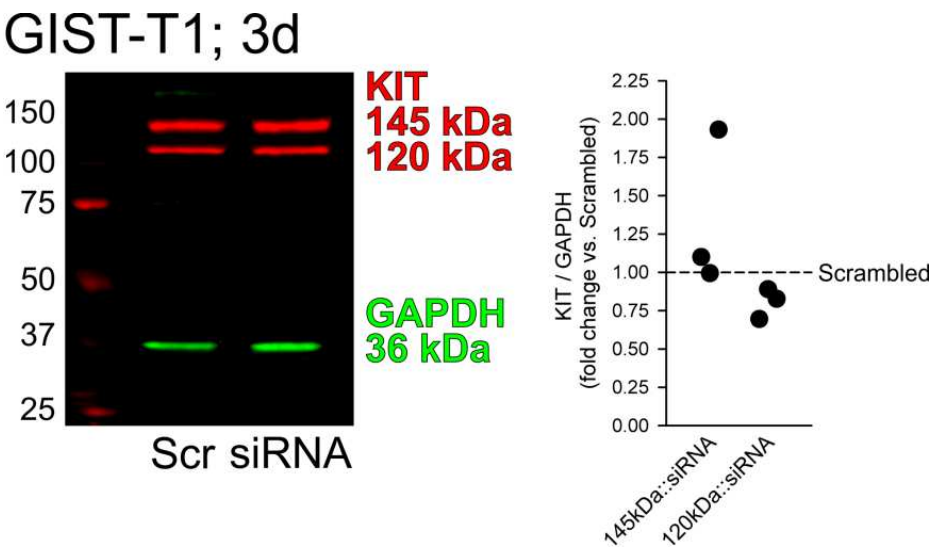

Supplementary Figure S3. Short-term RNAi-mediated PDGFRA knock-down did not reduce KIT protein levels in GIST-T1 cells. Representative immunoblot (left) and quantitative analysis (right) of KIT protein expression in GIST-T1 cells treated with PDGFRA-targeting siRNA or corresponding scrambled (Scr) sequences (25 nM) for 3 days (n=3/group). The profound downregulation of PDGFRA protein levels by the same treatments is demonstrated in the main text (**Figure 2*A***).

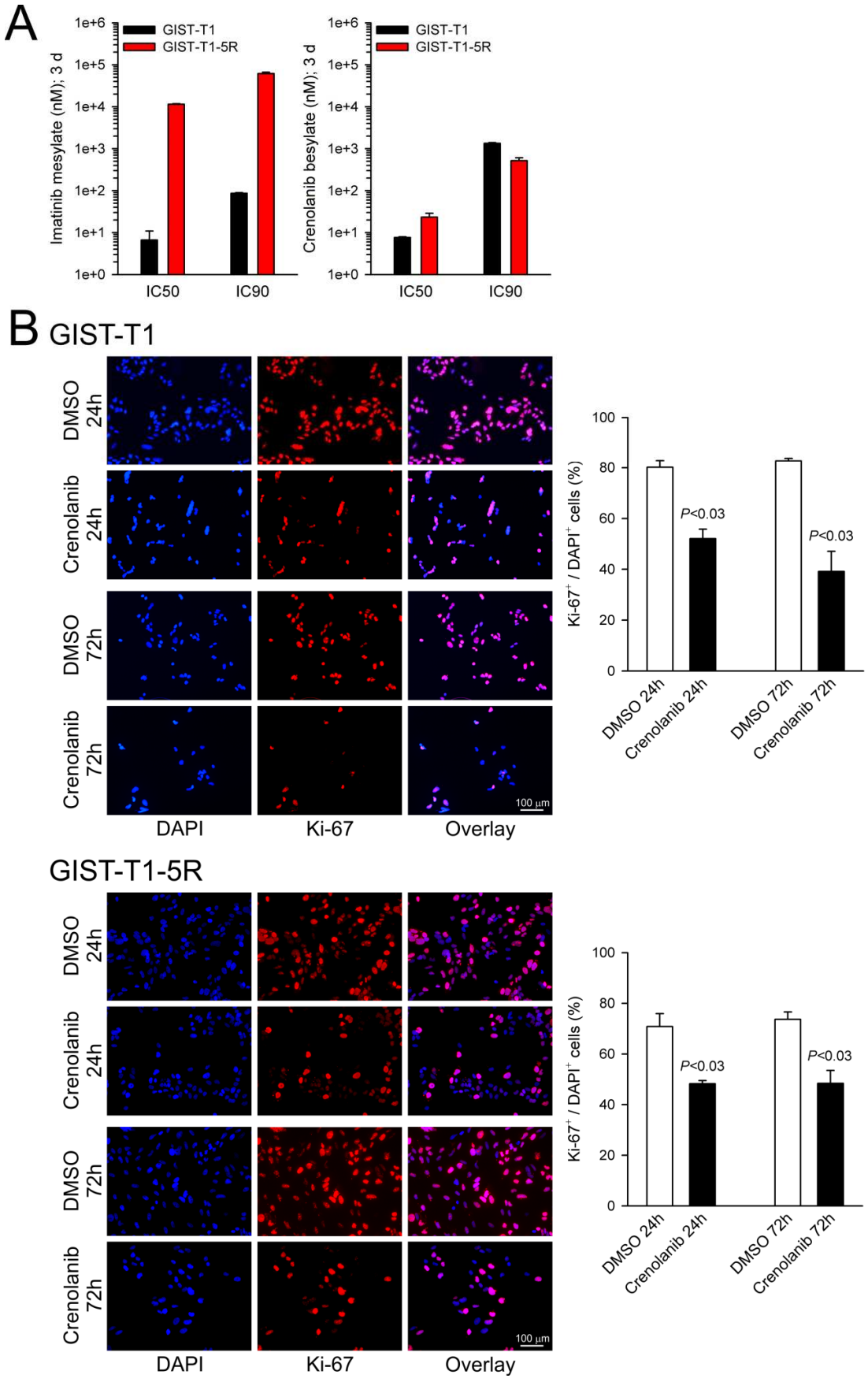
A
GIST-T1
GIST-T1-5R
Imatinib mesylate (nM); 3 d
Crenolanib besylate (nM); 3 d
1e+6
1e+5
1e+4
1e+3
1e+2
1e+1
1e+0
IC50
IC90
B GIST-T1
DMSO 24h
Crenolanib 24h
DMSO 72h
Crenolanib 72h
100 µm
DAPI
Ki-67
Overlay
Ki-67+ / DAPI+ cells (%)
P<0.03
P<0.03
DMSO 24h
Crenolanib 24h
DMSO 72h
Crenolanib 72h
GIST-T1-5R

Supplementary Figure S4. PDGFRA inhibition suppresses the proliferation of both imatinib-sensitive and imatinib-resistant, KIT^{+}PDGFRA^{+}, *KIT*-mutant GIST cells. (*A*) IC_{50} and IC_{90} values for imatinib and crenolanib from the MTS dose-response studies shown in **Figure 2*C***. Bars and error bars represent the mean and the standard error of the mean (SEM), respectively. Crenolanib inhibited the growth of the imatinib-resistant GIST-T1-5R cells and its imatinib-sensitive GIST-T1 parent line with comparable potency. (*B*) DAPI (blue) and Ki-67 immunofluorescence (red) detected in GIST-T1 and GIST-T1-5R cells following 24-h and 72-h treatment with 8.3 nM and 33.2 nM crenolanib, respectively. Proliferating cells identified by co-localization of Ki-67 immunoreactivity with the nuclear stain DAPI (purple color) are quantified in the bar graphs (mean and SEM; n=4/cell line/treatment/time point). *P* values are from Mann-Whitney rank sum tests. Crenolanib inhibited the proliferation of both the imatinib-sensitive GIST-T1 and the imatinib-resistant GIST-T1-5R cells.

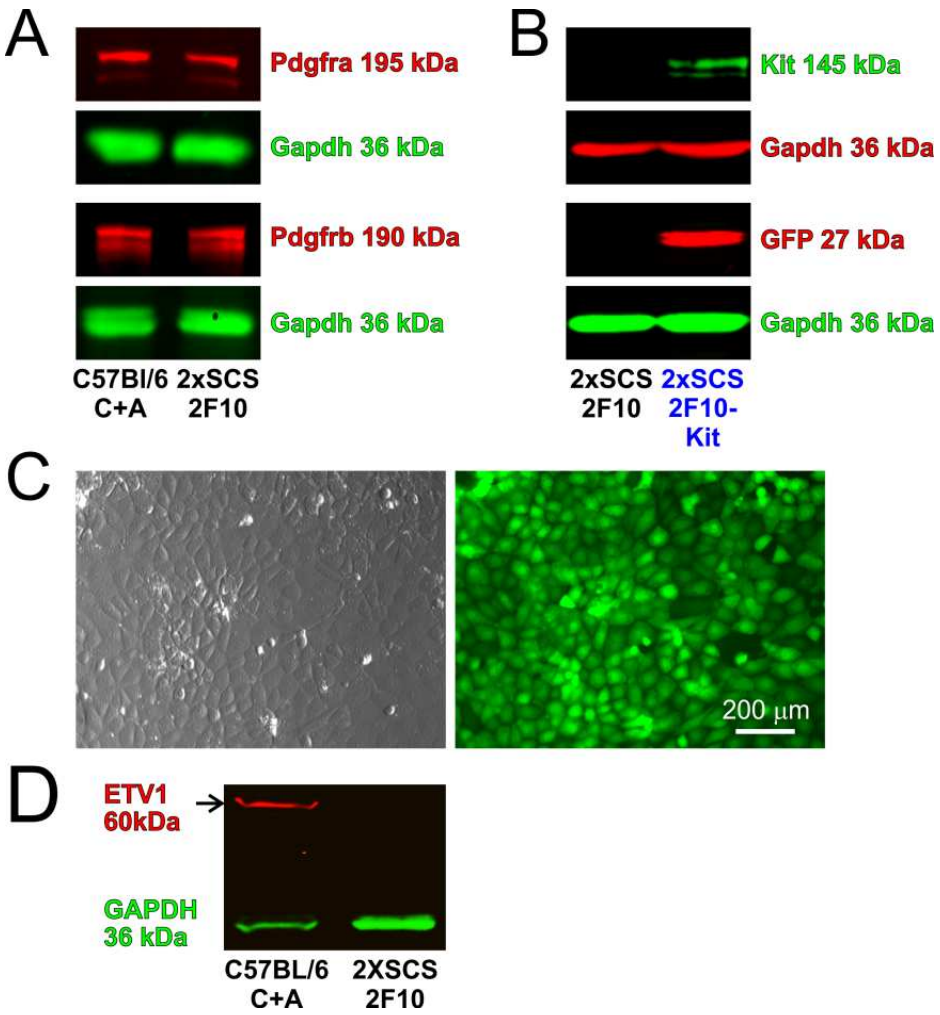

Supplementary Figure S5. Kit, Pdgfra, Pdgfrb and Etv1 expression in wild-type 2xSCS2F10 ICC-SC and 2xSCS2F10 cells retrovirally transduced to express Kit. (*A*) Wild-type 2xSCS2F10 cells expressed both Pdgfra and Pdgfrb by WB. C57Bl/6 C+A, gastric corpus and antrum *tunica muscularis* used as positive control. (*B*) 2xSCS2F10 cells transduced with the retroviral vector pMSCV-Kit-PIG {murine wild-type Kit–puromycin–IRES (internal ribosomal entry site)–GFP; 2xSCS2F10-Kit}, but not wild-type 2xSCS2F10 cells, expressed mouse Kit and GFP. (*C*) 2xSCS2F10-Kit cells uniformly expressed GFP from the retroviral vector as indicated by fluorescent microscopy (right panel). Left panel shows Hoffman modulation contrast image of the same field-of-view. Note epithelioid morphology characteristic of this cell line.[3] (*D*) Wild-

type 2xSCS2F10 cells did not express Etv1 protein. (*A*-*D*) Representative results from at least 3 experiments are shown.

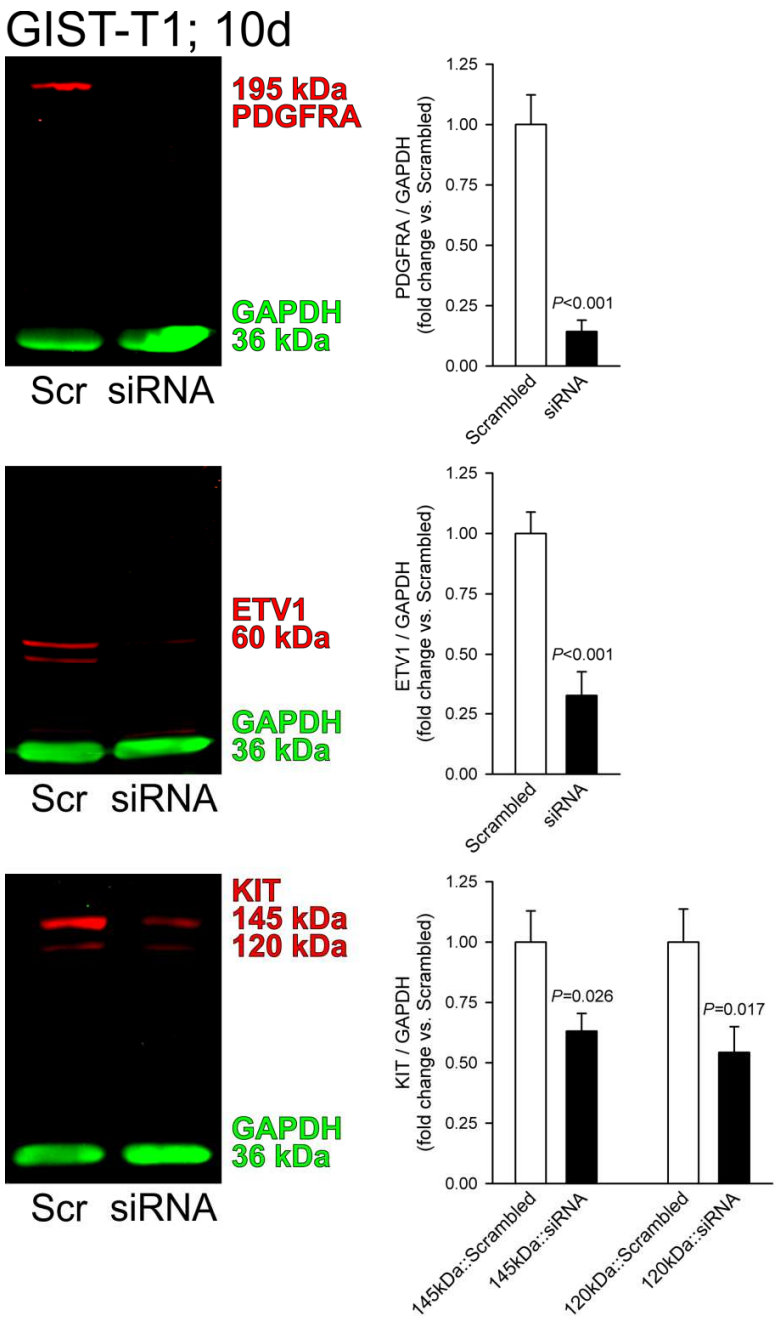

Supplementary Figure S6. Inhibition of ETV1 and KIT protein expression by long-term siRNA-mediated PDGFRA knock-down in GIST-T1 cells. Representative immunoblots (left) and quantitative analysis (right) of PDGFRA, ETV1 and KIT protein expression in GIST-T1 cells treated with PDGFRA-targeting siRNA or corresponding scrambled (Scr) sequences (25 nM) for 10 days (mean and SEM; n=12/group). *P* values are from Mann-Whitney rank sum tests.

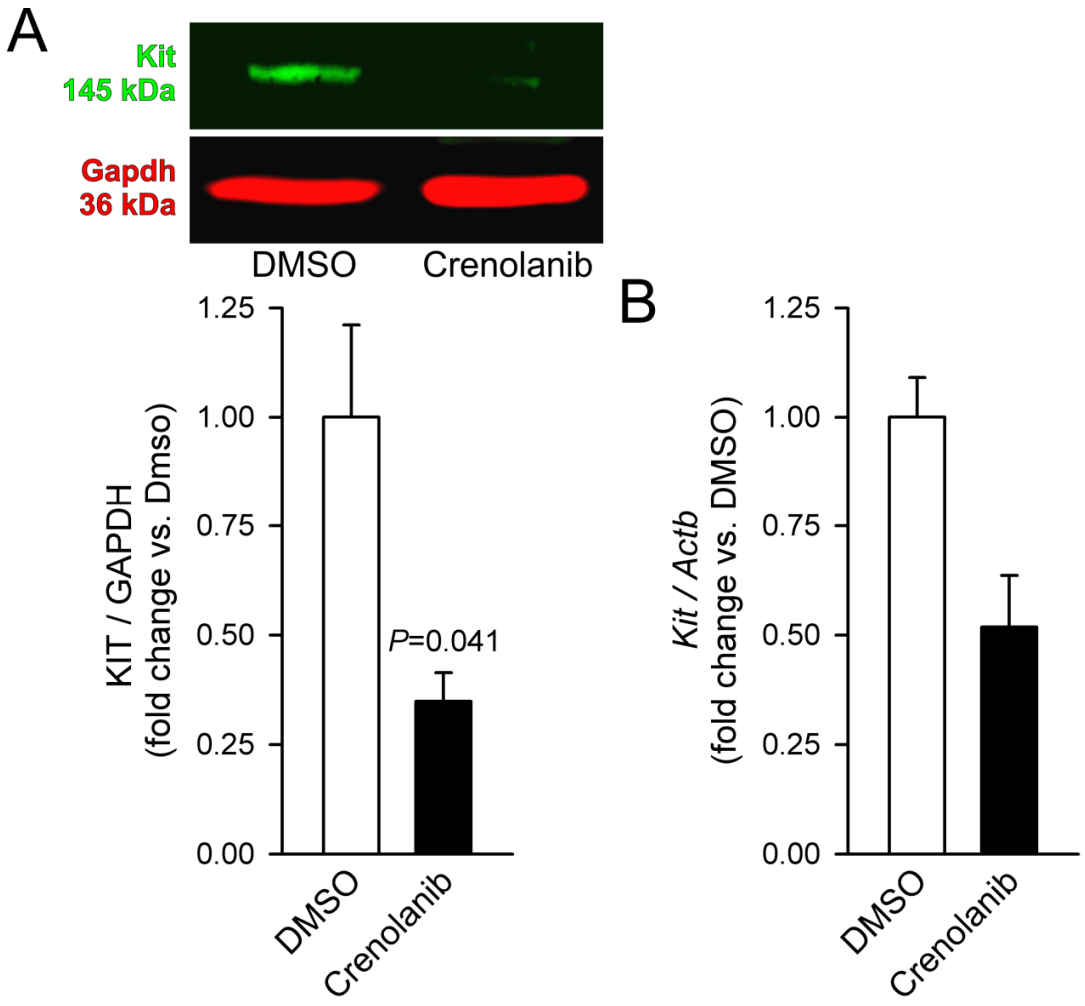

Supplementary Figure S7. Crenolanib inhibits Kit protein and mRNA expression in organotypic cultures of murine gastric corpus+antrum *tunica muscularis*. (*A*) Representative immunoblots (top) and quantitative analysis (bottom) of Kit protein expression in gastric *tunica muscularis* tissues maintained in organotypic cultures[11] in the presence of 16.6 nM crenolanib or DMSO vehicle for 30 days (mean and SEM; n=6/group). Media were changed every other day. *P* value is from Mann-Whitney rank sum test. (*B*) Expression of Kit mRNA in murine gastric *tunica muscularis* organotypic cultures prepared and maintained in an identical manner (mean and SEM; n=4/group). Ano1 mRNA did not change (not shown). Long-term exposure to crenolanib inhibited both Kit protein and mRNA.

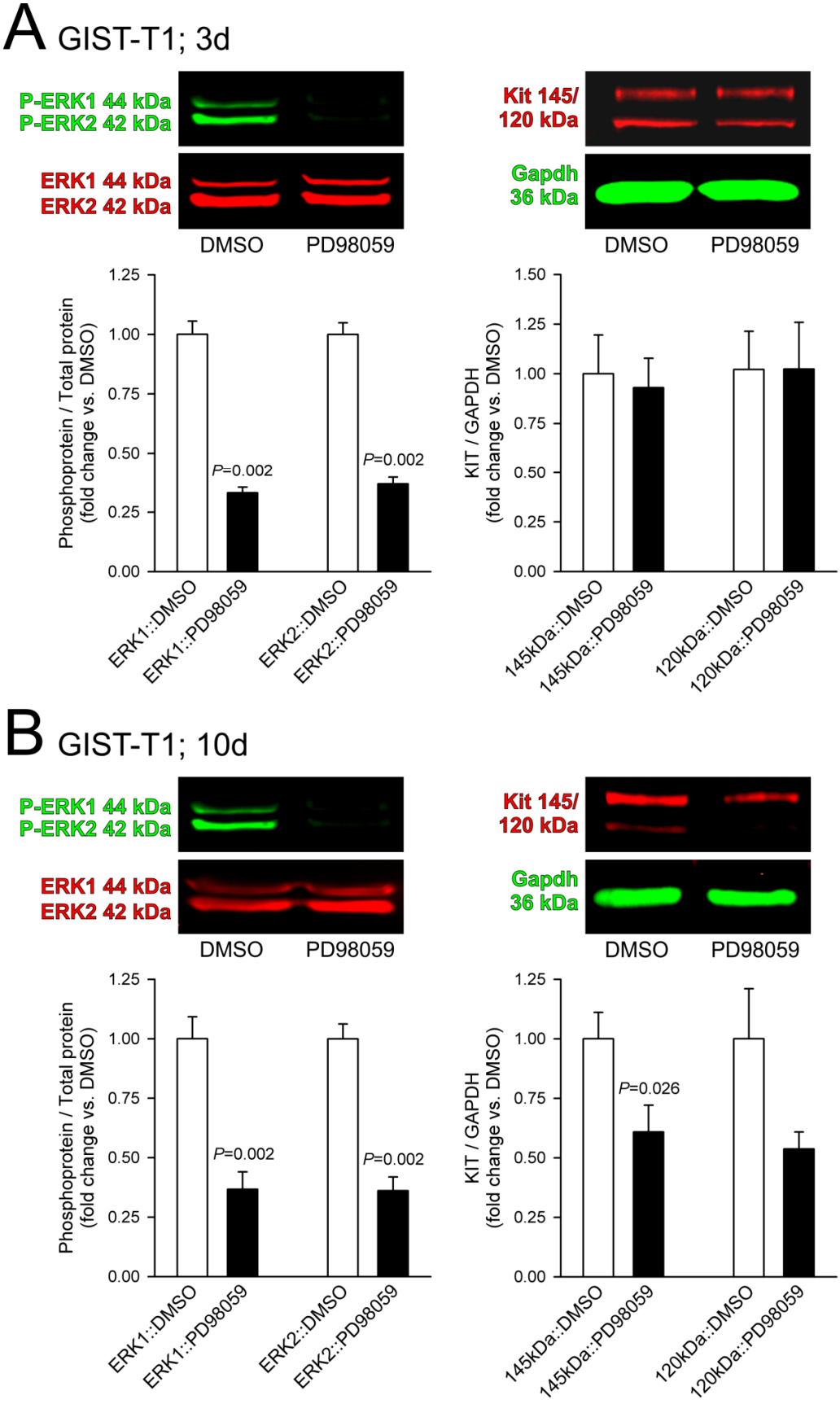
A GIST-T1; 3d
P-ERK1 44 kDa
P-ERK2 42 kDa
ERK1 44 kDa
ERK2 42 kDa
DMSO
PD98059
Kit 145/
120 kDa
Gapdh
36 kDa
DMSO
PD98059
Phosphoprotein / Total protein
(fold change vs. DMSO)
1.25
1.00
0.75
0.50
0.25
0.00
P=0.002
P=0.002
ERK1::DMSO
ERK1::PD98059
ERK2::DMSO
ERK2::PD98059
KIT / GAPDH
(fold change vs. DMSO)
1.50
1.25
1.00
0.75
0.50
0.25
0.00
145kDa::DMSO
145kDa::PD98059
120kDa::DMSO
120kDa::PD98059
B GIST-T1; 10d
P-ERK1 44 kDa
P-ERK2 42 kDa
ERK1 44 kDa
ERK2 42 kDa
DMSO
PD98059
Kit 145/
120 kDa
Gapdh
36 kDa
DMSO
PD98059
Phosphoprotein / Total protein
(fold change vs. DMSO)
1.25
1.00
0.75
0.50
0.25
0.00
P=0.002
P=0.002
ERK1::DMSO
ERK1::PD98059
ERK2::DMSO
ERK2::PD98059
KIT / GAPDH
(fold change vs. DMSO)
1.25
1.00
0.75
0.50
0.25
0.00
P=0.026
145kDa::DMSO
145kDa::PD98059
120kDa::DMSO
120kDa::PD98059

Supplementary Figure S8. Inhibition of KIT protein expression by long-term but not short-term inhibition of ERK1/2 MAPK activation in GIST-T1 cells. Representative immunoblots and quantitative analysis of ERK1/2 MAPK phosphorylation in GIST-T1 cells treated with the MAPK kinase inhibitor PD98059 (50μM) for 3 days (*A*) or 10 days (*B*) (mean and SEM; n=6/treatment/time point). *P* values are from Mann-Whitney rank sum tests. Media were changed after 5 days in the 10-day experiments.

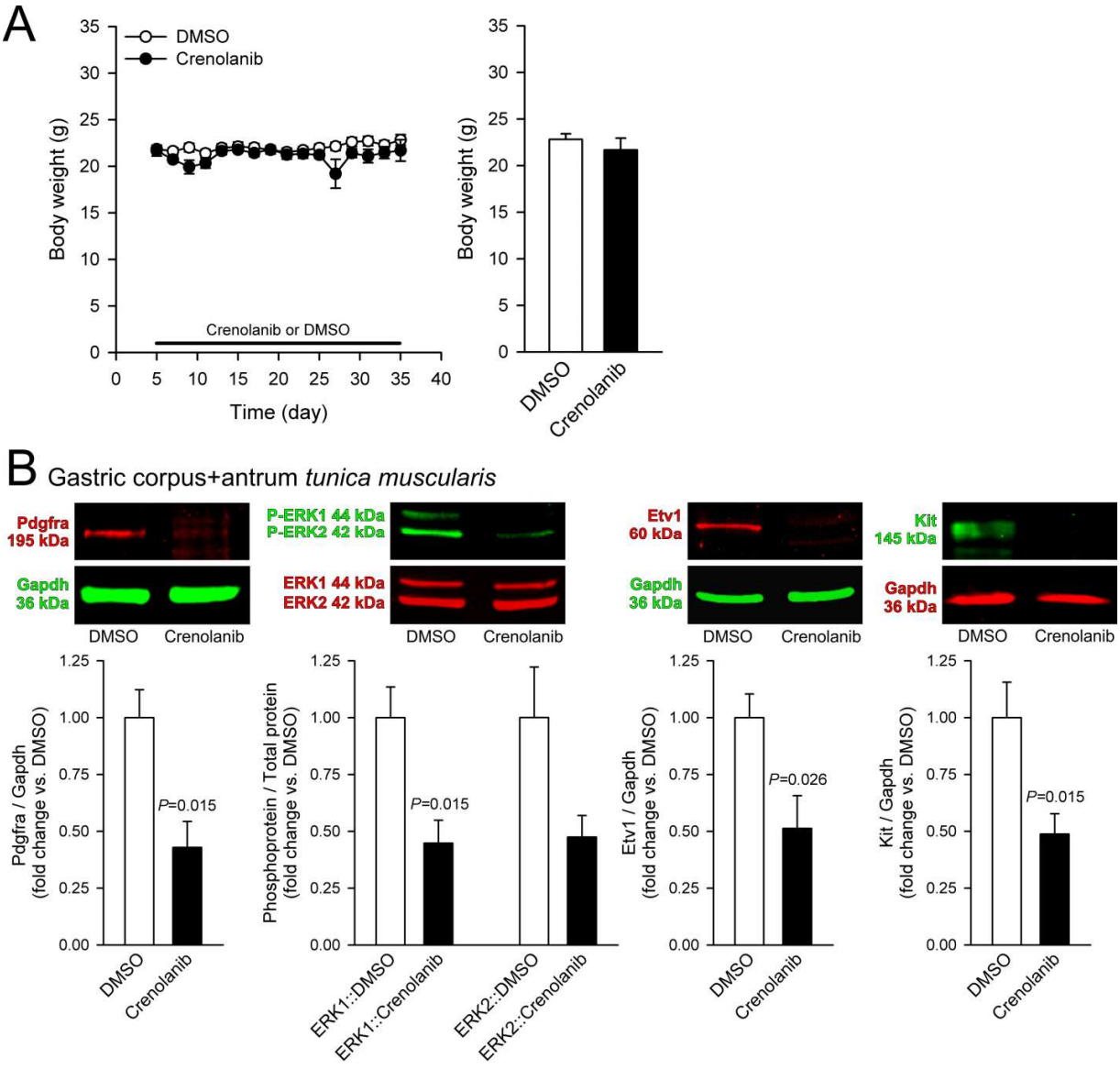

Supplementary Figure S9. Effects of crenolanib on body weights and corpus+antrum *tunica muscularis* protein expression in NCr-*nu/nu* mice transplanted with GIST-T1 cells. Tumor volumes, weights and protein expression are shown in **Figure 6** in the main text. (*A*) 12.5 mg/kg crenolanib administered intraperitoneally twice for 30 days did not reduce the body weights of NCr-*nu/nu* mice (mean and SEM; n=6 mice/group). (*B*) The same treatment significantly reduced Pdgfra, Etv1 and Kit protein expression and inhibited ERK1/2 MAPK

phosphorylation in the gastric *tunica muscularis* (mean and SEM; n=6/group). *P* values are from Mann-Whitney rank sum tests.

SUPPLEMENTARY REFERENCES

1. Gomez-Pinilla PJ, Gibbons SJ, Bardsley MR, et al. Ano1 is a selective marker of interstitial cells of Cajal in the human and mouse gastrointestinal tract. Am J Physiol Gastrointest Liver Physiol 2009;296:G1370-1381.
2. Asuzu DT, Hayashi Y, Izbeki F, et al. Generalized neuromuscular hypoplasia, reduced smooth muscle myosin and altered gut motility in the klotho model of premature aging. Neurogastroenterol Motil 2011;23:e309-323.
3. **Bardsley MR**, **Horvath VJ**, Asuzu DT, et al. Kitlow stem cells cause resistance to Kit/platelet-derived growth factor alpha inhibitors in murine gastrointestinal stromal tumors. Gastroenterology 2010;139:942-952.
4. **Izbeki F**, **Asuzu DT**, **Lorincz A**, et al. Loss of Kitlow progenitors, reduced stem cell factor and high oxidative stress underlie gastric dysfunction in progeric mice. J Physiol 2010;588:3101-3117.
5. Ro S, Park C, Jin J, et al. A model to study the phenotypic changes of interstitial cells of Cajal in gastrointestinal diseases. Gastroenterology 2010;138:1068-1078 e1061-1062.
6. Hamilton TG, Klinghoffer RA, Corrin PD, et al. Evolutionary divergence of platelet-derived growth factor alpha receptor signaling mechanisms. Mol Cell Biol 2003;23:4013-4025.
7. Hayashi Y, Asuzu DT, Gibbons SJ, et al. Membrane-to-nucleus signaling links insulin-like growth factor-1- and stem cell factor-activated pathways. PLoS One 2013;8:e76822.
8. Chou TC. Drug combination studies and their synergy quantification using the Chou-Talalay method. Cancer Res 2010;70:440-446.

9. Ordog T, Redelman D, Horowitz NN, et al. Immunomagnetic enrichment of interstitial cells of Cajal. Am J Physiol Gastrointest Liver Physiol 2004;286:G351-360.
10. Schwamb B, Pick R, Mateus Fernández SB, et al. FAM96A is a novel pro-apoptotic tumor suppressor in gastrointestinal stromal tumors. Int J Cancer 2015; in press.
11. Horvath VJ, Vittal H, Ordog T. Reduced insulin and IGF-I signaling, not hyperglycemia, underlies the diabetes-associated depletion of interstitial cells of Cajal in the murine stomach. Diabetes 2005;54:1528-1533.

Author names in bold designate shared co-first authors.